INTERACTIONS, CURRENTS, AND THE STRUCTURE OF FEW-NUCLEON SYSTEMS

R. SCHIAVILLA
Jefferson Lab, Newport News, VA 23606
and
Old Dominion University, Norfolk, VA 23529

Our current understanding of the structure of nuclei with $A \leq 8$, including energy spectra, electromagnetic form factors, and weak transitions, is reviewed within the context of a realistic approach to nuclear dynamics based on two- and three-nucleon interactions and associated electro-weak currents. Low-energy radiative and weak capture reactions of astrophysical relevance involving these light systems are also discussed.

1 Introduction

Few-nucleon systems provide a unique opportunity for testing the simple, traditional picture of the nucleus as a system of point-like nucleons interacting among themselves via effective many-body potentials, and with external electro-weak probes via effective many-body currents. Through advances in computational techniques and facilities, the last few years have witnessed dramatic progress in numerically exact studies of the structure and dynamics of systems with mass number $A \leq 8$, including energy spectra of low-lying states, momentum distributions and cluster amplitudes, elastic and inelastic electromagnetic form factors, β-decays, radiative and weak capture reactions at low energies, inclusive response to hadronic and electro-weak probes at intermediate energies.

In the present talk, I will review the "nuclear standard model" outlined above, and present the extent to which it is successful in predicting some of the nuclear properties alluded to earlier. Of course, given the limited time, some of the theoretical and experimental developments will be treated cursorily. Nevertheless, I still hope to be able to convey a broad view of the intriguing and important studies in few-nucleon physics today.

2 Potentials and Energy Spectra

The Hamiltonian in the nuclear standard model is written as

$$H = \sum_i K_i + \sum_{i<j} v_{ij} + \sum_{i<j<k} V_{ijk} \ , \tag{1}$$

where the kinetic energy operator K_i has charge-independent and charge-symmetry-breaking components due to the difference in proton and neutron masses, and v_{ij} and V_{ijk} are two- and three-nucleon potentials.

The two-nucleon potential consists of a long range part due to pion exchange, and a short-range part parameterized either in terms of heavy meson exchanges as, for example, in the Bonn potential [1], or via suitable operators and strength functions, as in the Argonne v_{18} (AV18) potential [2]. The short-range terms in these potentials are then constrained to fit *pp* and *np* scattering data up to energies of $\simeq 350$ MeV in the laboratory, and the deuteron binding energy. The modern models mentioned above provide fits to the Nijmegen data-base [3] characterized by χ^2 per datum very close to one, and should therefore be viewed as phase-equivalent. The AV18 model is most widely used; it has the form

$$\begin{aligned} v_{ij} &= v_{ij}^{\pi} + v_{ij}^{R} \\ &= \sum_{p=1,18} v^p(r_{ij})\, O_{ij}^p \ , \end{aligned} \tag{2}$$

where the first fourteen operators are isoscalar,

$$O_{ij}^{p=1-14} = \left[1, \sigma_i \cdot \sigma_j, S_{ij}, (\mathbf{L}\cdot\mathbf{S})_{ij}, \mathbf{L}^2, \mathbf{L}^2 \sigma_i \cdot \sigma_j, (\mathbf{L}\cdot\mathbf{S})_{ij}^2\right] \otimes \left[1, \tau_i \cdot \tau_j\right] \ , \tag{3}$$

while the last four isospin-symmetry-breaking operators have isovector and isotensor character,

$$O_{ij}^{p=15-18} = T_{ij} \ , \ \sigma_i \cdot \sigma_j T_{ij} \ , \ S_{ij} T_{ij} \ , (\tau_i + \tau_j)_z \ . \tag{4}$$

Here S_{ij} is the tensor operator, and T_{ij} is defined as $T_{ij} = 3\tau_{iz}\tau_{jz} - \tau_i \cdot \tau_j$. Unique among the modern potentials, the AV18 includes a fairly complete treatment of the electromagnetic interaction, since it retains, in addition to the leading Coulomb term, also contributions from magnetic moment interactions, vacuum polarization and two-photon exchange corrections. These terms, while typically very small (for example, in the deuteron the magnetic dipole-dipole interaction gives 18 keV extra repulsion [2]), need to be taken into account when very accurate predictions are required, as in the case, for

example, of studies of energy differences of isomultiplet states [4], or the cross section for proton weak capture on proton at keV energies [5].

It is now well established that two-nucleon potentials alone underbind nuclei [4]: for example, the AV18 and Bonn models give [6], in numerically exact calculations, binding energies of 24.28 MeV and 26.26 MeV respectively, which should be compared to the experimental value of 28.3 MeV. Moreover, ^{6}Li and ^{7}Li are unstable against breakup into αd and αt clusters, respectively, and that energy differences are not, in general, well predicted, when only two-nucleon potentials are retained in the Hamiltonian.

Important components of the three-nucleon potential arise from the internal structure of the nucleon. Since all degrees of freedom other than the nucleon have been integrated out, the presence of virtual Δ resonances, for example, induces three-nucleon potentials. They are written as

$$V_{ijk} = V_{ijk}^{2\pi} + V_{ijk}^{R} \ , \tag{5}$$

where $V^{2\pi}$ is the "long-range"term, resulting from the intermediate excitation of a Δ with pion exchanges involving the other two nucleons, known as the Fujita-Miyazawa term [7]. This term is present in all models, such as the Tucson-Melbourne potential [8] or the series of Urbana models [9]. The Urbana models parameterize V^R as

$$V^R = A^R \sum_{\text{cyclic } ijk} T_\pi^2(r_{ij}) T_\pi^2(r_{jk}) \ , \tag{6}$$

where $T_\pi(r)$ is the strength function of the pion-exchange tensor interaction. This term is meant to simulate the dispersive effects that are required when integrating out Δ degrees of freedom. The strengths of the Fujita-Miyazawa and dispersive terms are then determined, in the Urbana models, by fitting the triton binding energy and the saturation density of nuclear matter.

The Hamiltonian consisting of the AV18 two-nucleon and Urbana-IX three-nucleon potentials (AV18/UIX) predicts reasonably well the low-lying energy spectra of systems with $A \leq 8$ nucleons in "exact"Green's function Monte Carlo calculations [4]. The experimental binding energies of the α particle is exactly reproduced, while those of the A=6–8 systems are underpredicted by a few percent. This underbinding becomes (relatively) more and more severe as the neutron-proton asymmetry increases. An additional failure of this Hamiltonian model is the underprediction of spin-orbit splittings in the excitation spectra of these light systems. These failures have in fact led to the development of new three-nucleon interaction models [10]. These newly developed models, denoted as Illinois models, incorporate the Fujita-Miyazawa and

dispersive terms discussed above, but include in addition multipion exchange terms involving excitation of one or two Δ's, so-called pion-ring diagrams, as well as the terms arising from S-wave pion rescattering, required by chiral symmetry.

3 The Nuclear Electromagnetic Current

The nuclear current operator consists of one- and many-body terms that operate on the nucleon degrees of freedom:

$$\mathbf{j}(\mathbf{q}) = \sum_i \mathbf{j}_i^{(1)}(\mathbf{q}) + \sum_{i<j} \mathbf{j}_{ij}^{(2)}(\mathbf{q}) + \sum_{i<j<k} \mathbf{j}_{ijk}^{(3)}(\mathbf{q}) \ , \tag{7}$$

where $\mathbf{q}$ is the momentum transfer, and the one-body operator $\mathbf{j}_i^{(1)}$ has the standard expression in terms of single-nucleon convection and magnetization currents. The two-body current operator has "model-independent"and "model-dependent"components (for a review, see Ref. [11]). The model-independent terms are obtained from the charge-independent part of the AV18, and by construction satisfy current conservation with this interaction. The leading operator is the isovector "π-like"current obtained from the isospin-dependent spin-spin and tensor interactions. The latter also generate an isovector "ρ-like "current, while additional model-independent isoscalar and isovector currents arise from the central and momentum-dependent interactions. These currents are short-ranged and numerically far less important than the π-like current. Finally, models for three-body currents have been derived in Ref. [12], however the associated contributions have been found to be very small in studies of the magnetic structure of the trinucleons [12].

The model-dependent currents are purely transverse and therefore cannot be directly linked to the underlying two-nucleon interaction. Among them, those associated with the Δ-isobar are the most important ones in the momentum-transfer regime being discussed here. These currents are treated within the transition-correlation-operator (TCO) scheme [12,13], a scaled-down approach to a full $N+\Delta$ coupled-channel treatment. In the TCO scheme, the Δ degrees of freedom are explicitly included in the nuclear wave functions by writing

$$\Psi_{N+\Delta} = \left[\mathcal{S} \prod_{i<j} \left(1 + U_{ij}^{TR}\right) \right] \Psi \ , \tag{8}$$

where Ψ is the purely nucleonic component, $\mathcal{S}$ is the symmetrizer and the transition correlations U_{ij}^{TR} are short-range operators, that convert NN pairs into $N\Delta$ and $\Delta\Delta$ pairs. In the results reported here, the Ψ is taken from CHH solutions of the AV18/UIX Hamiltonian with nucleons only interactions, while the U_{ij}^{TR} is obtained from two-body bound and low-energy scattering state solutions of the full N-Δ coupled-channel problem. Both $\gamma N\Delta$ and $\gamma\Delta\Delta$ M_1 couplings are considered with their values, $\mu_{\gamma N\Delta} = 3$ n.m. and $\mu_{\gamma\Delta\Delta} = 4.35$ n.m., obtained from data [13].

4 The *pd* Radiative Capture

There are now available many high-quality data, including differential cross sections, vector and tensor analyzing powers, and photon polarization coefficients, on the *pd* radiative capture at c.m. energies ranging from 0 to 2 MeV [14,15,16,17]. These data indicate that the reaction proceeds predominantly through S- and P-wave capture. The aim here is to verify the extent to which they can be described satisfactorily by a calculation based on a realistic Hamiltonian (the AV18/UIX model) and a current operator constructed consistently with the two- and three-nucleon interactions [18].

The predicted angular distributions of the differential cross section $\sigma(\theta)$, vector and tensor analyzing powers $A_y(\theta)$ and $T_{20}(\theta)$, and photon linear polarization coefficient $P_\gamma(\theta)$ are compared with the TUNL data below 50 keV from Refs. [14,16] in Fig 1. The agreement between the full theory, including many-body current contributions, and experiment is generally good. However, a closer inspection of the figure reveals the presence of significative discrepancies between theory and experiment in the small angle behavior of $\sigma(\theta)$ and $T_{20}(\theta)$, as well as in the S-factor below 40 keV [18]. The S-wave capture proceeds mostly through the M_1 transitions connecting the doublet and quartet *pd* states to ^{3}He–the associated reduced matrix elements (RMEs) are denoted by m_2 and m_4, respectively. The situation for P-wave capture is more complex, although at energies below 50 keV it is dominated by the E_1 transitions from the doublet and quartet *pd* states having channel spin S=1/2, whose RMEs I denote as p_2 and p_4. The E_1 transitions involving the channel spin $S = 3/2$ states, while smaller, do play an important role in $T_{20}(\theta)$.

The TUNL [16] and Wisconsin [17] groups have determined the leading M_1 and E_1 RMEs via fits to the measured observables. The results of this fitting procedure are compared with the calculated RMEs in Table 1. The phase of each RME is simply related to the elastic *pd* phase shift [17], which at these low energies is essentially the Coulomb phase shift. As can be seen from Table 1, the most significant differences between theoretical and experimental RMEs

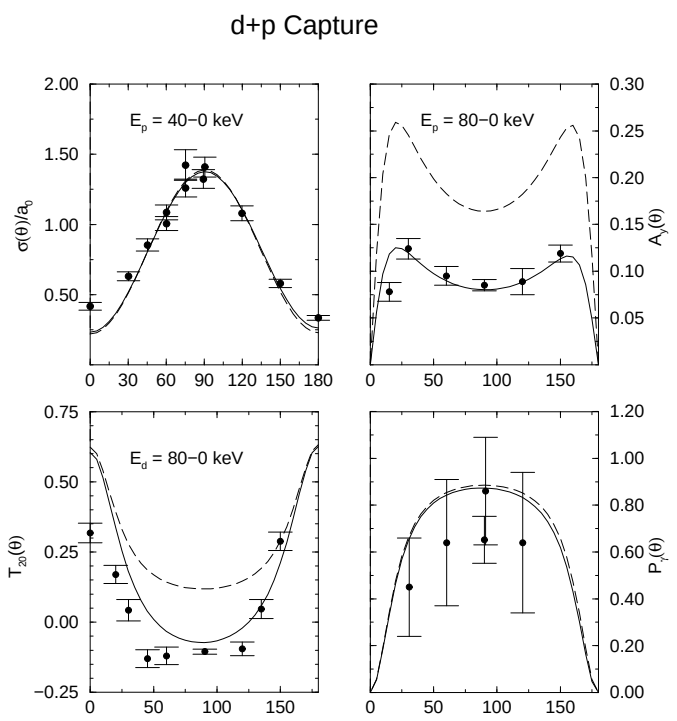

Figure 1. The energy integrated cross section $\sigma(\theta)/a_0$ ($4\pi a_0$ is the total cross section), vector analyzing power $A_y(\theta)$, tensor analyzing power $T_{20}(\theta)$ and photon linear polarization coefficient $P_\gamma(\theta)$ obtained with the AV18/UIX Hamiltonian model and one-body only (dashed line) or both one- and many-body (solid line) currents are compared with the experimental results of Ref. [14].

are found for $|p_4|$. The theoretical overprediction of p_4 is the cause of the discrepancies mentioned above in the low-energy ($\leq$ 50 keV) S-factor and small angle $\sigma(\theta)$.

It is interesting to analyze the ratio $r_{E1} \equiv |p_4/p_2|^2$. Theory gives $r_{E1} \simeq 1$, while from the fit it results that $r_{E1} \approx 0.74 \pm 0.04$. It is important to stress that the calculation of these RMEs is not influenced by uncertainties in the two-body currents, since their values are entirely given by the long-wavelength form of the E_1 operator (Siegert's theorem), which has no spin-dependence (for a thorough discussion of the validity of the long-wavelength approximation in E_1 transitions, particularly suppressed ones, see Ref. [18]). It is therefore of interest to examine more closely the origin of the above discrepancy. If the interactions between the p and d clusters are switched off, the relation $r_{E1} \simeq 1$ then simply follows from angular momentum algebra. Deviations of this ratio from one are therefore to be ascribed to differences induced by the interactions in the S=1/2 doublet and quartet wave functions. The AV18/UIX interactions in these channels do not change the ratio above significantly. It should be emphasized that the studies carried out up until now ignore, in the continuum states, the effects arising from electromagnetic interactions beyond the static

Coulomb interaction between protons. It is not clear whether the inclusion of these long-range interactions, in particular their spin-orbit component, could explain the splitting between the p_2 and p_4 RMEs observed at very low energy. This discrepancy seems to disappear at 2 MeV [18].

Table 1. Magnitudes of the leading M_1 and E_1 RMEs for pd capture at $E_p = 40$ keV.

RME	IA	FULL	FIT
$\|m_2\|$	0.172	0.322	0.340±0.010
$\|m_4\|$	0.174	0.157	0.157±0.007
$\|p_2\|$	0.346	0.371	0.363±0.014
$\|p_4\|$	0.343	0.378	0.312±0.009

Finally, the doublet m_2 RME is underpredicted by theory at the 5 % level. On the other hand, the cross section for nd capture at thermal neutron energy is calculated to be 578 μb with the AV18/UIX model, which is 15 % larger than the experimental value (508±15) μb [19]. Of course, M_1 transitions, particularly doublet ones, are significantly influenced by many-body current contributions. Indeed, an analysis of the isoscalar (μ_S) and isovector (μ_V) magnetic moments of the trinucleons [12] suggests that the present model for the isoscalar two-body currents, constructed from the AV18 spin-orbit and quadratic-momentum dependent interactions, tends to overestimate μ_S by about 5 %. The experimental value for μ_V, however, is almost perfectly reproduced. It appears that the present model for two-body currents needs to be improved.

5 The Nuclear Weak Current and the $p\,^3$He Weak Capture

The nuclear weak current and charge operators consist of vector and axial-vector parts, with corresponding one- and many-body components. The weak vector current and charge are constructed from the corresponding (isovector) electromagnetic terms, in accordance with the conserved-vector-current hypothesis, and thus have [20] "model-independent"and "model-dependent"components. The former are determined by the interactions, the latter include the transverse currents associated with Δ excitation.

The leading many-body terms in the axial current, in contrast to the case of the weak vector (or electromagnetic) current, are those due to Δ excitation, which are treated within the TCO scheme, discussed above. The axial charge operator includes the long-range pion-exchange term [21], required by low-energy theorems and the partially-conserved-axial-current relation, as

well as the (expected) leading short-range terms constructed from the central and spin-orbit components of the nucleon-nucleon interaction [22].

The largest model dependence is in the weak axial current. The $N\Delta$ axial coupling constant g_A^* is not well known. In the quark-model, it is related to the axial coupling constant of the nucleon by the relations $g_A^* = (6\sqrt{2}/5)g_A$. This value has often been used in the literature in the calculation of Δ-induced axial current contributions to weak transitions. However, given the uncertainties inherent to quark-model predictions, a more reliable estimate for g_A^* is obtained by determining its value phenomenologically. It is well established by now [5] that one-body axial currents lead to a $\simeq$ 4 % underprediction of the measured Gamow-Teller matrix element in tritium β-decay. This small 4 % discrepancy can then be used to determine g_A^* [20]. While this procedure is inherently model dependent, its actual model dependence is in fact very weak, as has been shown in Ref. [5].

The calculated values for the astrophysical S-factor in the energy range 0–10 keV are listed in Table 2 [20]. Inspection of the table shows that: (i) the energy dependence is rather weak, the value at 10 keV is only about 4 % larger than that at 0 keV; (ii) the P-wave capture states are found to be important, contributing about 40 % of the calculated S-factor. However, the contributions from D-wave channels are expected to be very small, as explicitly verified in ^{3}D$_1$ capture. (iii) The many-body axial currents associated with Δ excitation play a crucial role in the (dominant) ^{3}S$_1$ capture, where they reduce the S-factor by more than a factor of four; thus the destructive interference between the one- and many-body current contributions, obtained in Ref. [13], is confirmed in the study of Ref. [20], based on more accurate wave functions. The (suppressed) one-body contribution comes mostly from transitions involving the D-state components of the ^{3}He and ^{4}He wave functions, while the many-body contributions are predominantly due to transitions connecting the S-state in ^{3}He to the D-state in ^{4}He, or viceversa.

Table 2. The *hep* S-factor, in units of 10^{-20} keV b, calculated with CHH wave functions corresponding to the AV18/UIX Hamiltonian model, at $p\,^3$He c.m. energies E=0, 5, and 10 keV. The rows labelled "one-body"and "full"list the contributions obtained by retaining the one-body only and both one- and many-body terms in the nuclear weak current. The contributions due the ^{3}S$_1$ channel only and all S- and P-wave channels are listed separately.

	E=0 keV		E=5 keV		E=10 keV	
	^{3}S$_1$	S+P	^{3}S$_1$	S+P	^{3}S$_1$	S+P
one-body	26.4	29.0	25.9	28.7	26.2	29.3
full	6.38	9.64	6.20	9.70	6.36	10.1

The chief conclusion of Ref. [20] is that the *hep* S-factor is predicted to be $\simeq$ 4.5 times larger than the value adopted in the standard solar model (SSM) [23]. This enhancement, while very significant, is smaller than that first suggested in Ref. [24]. Even though this result is inherently model dependent, it is unlikely that the model dependence is large enough to accommodate a drastic increase in the value obtained here. Indeed, calculations using Hamiltonians based on the AV18 two-nucleon interaction only and the older AV14/UVIII two- and three-nucleon interactions [25] predict zero energy S-factor values of 12.1×10^{-20} keV b and 10.2×10^{-20} keV b, respectively. It should be stressed, however, that the AV18 model, in contrast to the AV14/UVIII, does not reproduce the experimental binding energies and low-energy scattering parameters of the three- and four-nucleon systems. The AV14/UVIII prediction is only 6 % larger than the AV18/UIX zero-energy result. This 6 % variation should provide a fairly realistic estimate of the theoretical uncertainty due to the model dependence. The precise calculation of the S-factor and the consequent absolute prediction for the *hep* neutrino flux should allow much greater discrimination among proposed solar neutrino oscillation solutions [20].

6 Conclusions and Acknowledgments

Improvements in the modeling of two- and three-nucleon interactions and nuclear electro-weak currents, and the significant progress made in the last few years in the description of bound and continuum wave functions, make it now possible to perform first-principle calculations of interesting nuclear properties of light nuclei. Experimentally known electromagnetic and weak transitions of systems in the mass range $2 \leq A \leq 8$ provide powerful constraints on models of nuclear currents.

I wish to thank J. Carlson, A. Kievsky, L.E. Marcucci, V.R. Pandharipande, S.C. Pieper, D.O. Riska, S. Rosati, M. Viviani, and R.B. Wiringa for their many important contributions to the work reported here. This work was supported by DOE contract DE-AC05-84ER40150 under which the Southeastern Universities Research Association (SURA) operates the Thomas Jefferson National Accelerator Facility.

References

1. R. Machleidt, F. Sammarruca, and Y. Song, Phys. Rev. C **53**, R1483 (1996); R. Machleidt, nucl-th/0006014.
2. R.B. Wiringa, V.G.J. Stoks, and R. Schiavilla, Phys. Rev. C **51**, 38 (1995).

3. J.R. Bergervoet *et al.*, Phys. Rev. C **41**, 1435 (1990); V.G.J. Stoks, R.A.M. Klomp, M.C.M. Rentmeester, and J.J. de Swart, Phys. Rev. C **48**, 792 (1993).
4. R.B. Wiringa, S.C. Pieper, J. Carlson, and V.R. Pandharipande, Phys. Rev. C **62**, 014001 (2000).
5. R. Schiavilla *et al.*, Phys. Rev. C **58**, 1263 (1998).
6. A. Nogga, H. Kamada, and W. Glöckle, Phys. Rev. Lett. **85**, 944 (2000).
7. J. Fujita and H. Miyazawa, Prog. Theor. Phys. **17**, 360 (1957).
8. S.A. Coon *et al.*, Nucl. Phys. **A317**, 242 (1979).
9. B.S. Pudliner, V.R. Pandharipande, J. Carlson, and R.B. Wiringa, Phys. Rev. Lett. **74**, 4396 (1995).
10. J. Carlson, V.R. Pandharipande, S.C. Pieper, and R.B. Wiringa, private communication.
11. J. Carlson and R. Schiavilla, Rev. Mod. Phys. **70**, 743 (1998).
12. L.E. Marcucci, D.O. Riska, and R. Schiavilla, Phys. Rev. C **58**, 3069 (1998).
13. R. Schiavilla, R.B. Wiringa, V.R. Pandharipande, and J. Carlson, Phys. Rev. C **45**, 2628 (1992).
14. G.J. Schmid *et al.*, Phys. Rev. Lett. **76**, 3088 (1996).
15. L. Ma *et al.*, Phys. Rev. C **55**, 588 (1997).
16. E.A. Wulf *et al.*, Phys. Rev. C **61**, 021601(R) (1999).
17. M.K. Smith and L.D. Knutson, Phys. Rev. Lett. **82**, 4591 (1999).
18. M. Viviani, A. Kievsky, L.E. Marcucci, S. Rosati, and R. Schiavilla, Phys. Rev. C **61**, 064001 (2000).
19. E.T. Jurney, P.J. Bendt, and J.C. Browne, Phys. Rev. C **25**, 2810 (1982).
20. L.E. Marcucci, R. Schiavilla, M. Viviani, A. Kievsky, and S. Rosati, Phys. Rev. Lett. **84**, 5959 (2000); L.E. Marcucci, R. Schiavilla, M. Viviani, A. Kievsky, S. Rosati, and J.F. Beacom, nucl-th/0006005, Phys. Rev. C. in press.
21. K. Kubodera, J. Delorme, and M. Rho, Phys. Rev. Lett. **40**, 755 (1978).
22. M. Kirchbach, D.O. Riska, and K. Tsushima, Nucl. Phys. **A542**, 616 (1992).
23. J.N. Bahcall, S. Basu, and M.H. Pinsonneault, Phys. Lett. B **433**, 1 (1998).
24. J.N. Bahcall and P.I. Krastev, Phys. Lett. B **436**, 243 (1998).
25. R.B. Wiringa, R.A. Smith, and T.L. Ainsworth, Phys. Rev. C **29**, 1207 (1984); R.B. Wiringa, Phys. Rev. C **43**, 1585 (1991).